

Article

Waste Heat Driven Multi-Ejector Cooling Systems: Optimization of Design at Partial Load; Seasonal Performance and Cost Evaluation

Luca Viscito , Gianluca Lillo, Giovanni Napoli and Alfonso William Mauro *

Department of Industrial Engineering, Federico II University of Naples P. le Tecchio 80, 80125 Naples, Italy; luca.viscito@unina.it (L.V.); gianluca.lillo@unina.it (G.L.); giovanni.napoli@unina.it (G.N.)

* Correspondence: wmauro@unina.it

Abstract: In this paper, a seasonal performance analysis of a hybrid ejector cooling system is carried-out, by considering a multi-ejector pack as expansion device. A 20 kW ejector-based chiller was sized to obtain the optimal tradeoff between performance and investment costs. The seasonal performance of the proposed solution was then evaluated through a dynamic simulation able to obtain the performance of the designed chiller with variable ambient temperatures for three different reference climates. The optimized multi-ejector system required three or four ejectors for any reference climate and was able to enhance the system performance at partial load, with a significant increase (up to 107%) of the seasonal energy efficiency ratio. The proposed system was then compared to conventional cooling technologies supplied by electric energy (electrical chillers EHP) or low-grade heat sources (absorption chillers AHP) by considering the total costs for a lifetime of 20 years and electric energy-specific costs for domestic applications from 0.10 to 0.50 €/kWhel. The optimized multi-ejector cooling system presented a significant convenience with respect to both conventional technologies. For warmer climates and with high electricity costs, the minimum lifetime for the multi-ejector system to achieve the economic break-even point could be as low as 1.9 years.

Keywords: thermo-economic analysis; seasonal performance; dynamic simulation; multi-ejector; heat driven cooling systems



Citation: Viscito, L.; Lillo, G.; Napoli, G.; Mauro, A.W. Waste Heat Driven Multi-Ejector Cooling Systems: Optimization of Design at Partial Load; Seasonal Performance and Cost Evaluation. *Energies* **2021**, *14*, 5663. <https://doi.org/10.3390/en14185663>

Academic Editor: Andrea Frazzica

Received: 22 July 2021

Accepted: 7 September 2021

Published: 9 September 2021

Publisher's Note: MDPI stays neutral with regard to jurisdictional claims in published maps and institutional affiliations.



Copyright: © 2021 by the authors. Licensee MDPI, Basel, Switzerland. This article is an open access article distributed under the terms and conditions of the Creative Commons Attribution (CC BY) license (<https://creativecommons.org/licenses/by/4.0/>).

1. Introduction

The rapid growth of the global population, especially in developing countries, will lead to an increase in global energy demand equal to 37% between 2014 and 2040, as reported by the International Energy Agency [1]. Consequently, carbon dioxide emissions will rise up to 20% in the same period, with an increase of 3.6 °C in the global average temperature [1]. According to studies by the International Energy Agency (2010) [2], the building sector is one of the most energy-consuming fields, with CO₂ emissions expected to nearly double and global final energy demand forecast to increase as much as 60% by 2050. In the European Union, half of the energy consumption is related to heating and cooling demand in buildings and industries [3]; meanwhile, in household applications, 79% of total energy for final use is for heating and hot water purposes (192.5 Mtoe). A reduction in primary energy associated with the civil sector could be obtained by increasing the use of renewable sources for two purposes: producing electric energy to power cooling systems, and directly using heat power to supply heat-driven cooling systems. Great efforts have been made to increase the role of renewable sources in electricity production; according to the International Energy Agency (2015) [4], the energy supplied by renewable sources for worldwide electric energy production was about 23.3%; and higher percentages, of 31.3% and 33.9%, were respectively attained in the European Union (2017) [4] and Italy (2018) [5]. However, to our knowledge, the direct use of heat from renewable sources or waste heat on a large scale for space air conditioning during the summer season has not yet

been investigated. Moreover, considering the ongoing increase in the cost of electric energy to feed conventional electric devices for space heating/cooling, heat-driven systems could represent an attractive alternative solution for residential and commercial space cooling applications. Among the already-available solutions on the market, such as absorption and combined ORC/VCC plants, hybrid ejector systems seem to be more suitable for small-capacity applications due to their reduced complexity and lower specific costs when compared to conventional heat driven systems.

As reviewed by Besagni et al. [6], the scientific literature on hybrid ejector cooling systems has been focused on the selection of an appropriate working fluid. Sun [7] used a numerical approach to compare the performance of ejector cooling systems by employing 11 working fluids. The author obtained the best outcomes with R152a (COP values up to 0.50) and R500 (COP values up to 0.47). The recent work of Kasperski and Gil [8] has theoretically analyzed several hydrocarbons, and the optimal vapor generator temperature was calculated for each fluid. In terms of system performance, the highest COP of 0.32 was obtained with R600a at a generator temperature of 102 °C; meanwhile, using R601 as the working fluid, a COP of 0.27 was obtained at 165 °C. Chen et al. [9] compared different types of fluids (wet, dry and isentropic) to verify their usefulness in an ejector cooling system. Several refrigerants (R236fa, R245ca and R245fa among them) were investigated in the work of Gil and Kasperki [10] for $T_{gv} = 200$ °C. The results demonstrated that none of the investigated working fluids could cover the whole operating range with good performance, due to the existence of an optimal T_{gv} maximizing entrainment ratio and COP. A maximum value of COP equal to 0.23 was obtained with R236fa at 95 °C. In the range from 105 °C to 125 °C, R236ea yielded the highest COP, of 0.21. The fluid R123 provided the best performance when the maximum temperature was 125 °C.

Lillo et al. [11] proposed a comparison, using a thermo-economic analysis, between a hybrid ejector cooling system and conventional heat-driven cooling technologies such as absorption and combined ORC/VCC plants. Several working fluids including HFCs, HFOs, hydrocarbons and ammonia were investigated, and ammonia solutions were found to be the most efficient and less expensive options. Furthermore, the cost-performance comparison showed that ejector systems provide a lower COP at costs similar to those of single-effect absorption chillers. However, when considering small-scale applications, high specific costs associated with absorption chillers make the hybrid ejector a potentially competitive cooling technology.

For an accurate comparison between hybrid ejector cooling systems and other cooling technologies, real operating conditions (accounting for the variation in boundary conditions during a typical cooling season) should be considered. Regarding the ejector cooling cycle, assuming a constant heat source and chilled water temperature, the main parameter affecting system operating conditions is the external ambient temperature, and hence, the condensing temperature. The condensing temperature significantly influences the entrained mass flow rate, as shown in Figure 1, with potentially a very low entrainment ratio or failure in ejector operation when the operating pressure is below the critical value to obtain a choked flow. Since the mass flow rate is influenced by the variation in the boundary conditions, the ejector cannot work with acceptable performance under partial load, and therefore, a single ejector with fixed geometry is not able to handle the cooling load under variable operating conditions.

In fact, the analysis presented by Sun [12] pointed out the limits of the use of ejectors having fixed geometry in refrigeration plants due to low system performance (approximately 0.2–0.3), and the problem in obtaining high efficiencies under off-design operating conditions. Therefore, the use of a device able to adjust the ejector geometry according to variations in operating conditions is needed. The scientific literature has proposed variable-geometry ejectors having a movable spindle that varies the motive nozzle throat section, as experimentally investigated by Pereira et al. [13] in a 1.6 kW cooling system. By changing the spindle position, the primary flow rate could vary up to 80%, with COP values ranging between 0.45 and 0.88. Improved COP values of up to 85% were obtained, and the existence

of an optimal spindle position as a function of operating conditions was demonstrated. Van Nguyen et al. [14] presented an experimental study of a solar heat driven ejector air-conditioning system, evaluating the influence of the ejector geometry on system performance. The results clearly indicated the benefit of using the variable-geometry ejector, with a COP improvement equal to 24% (maximum of 0.29).

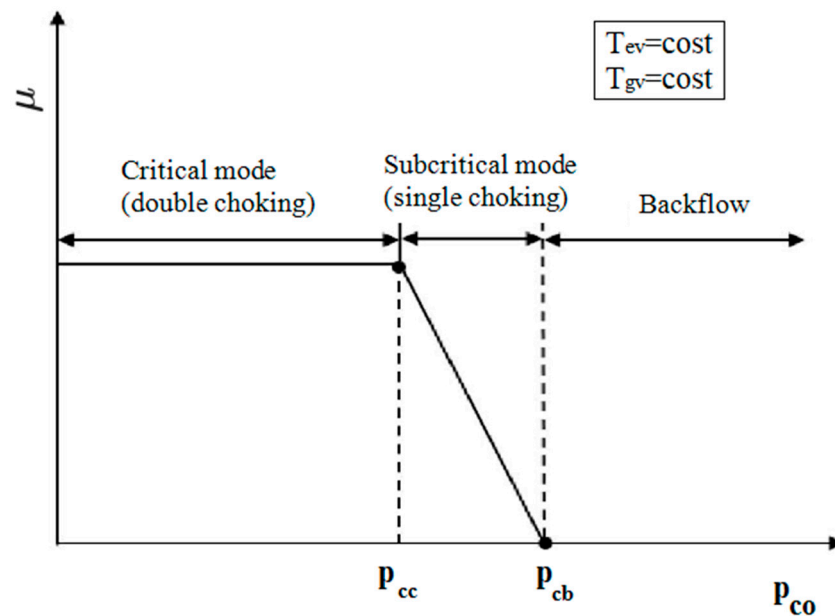


Figure 1. Operating modes of vapor ejector with fixed ejector geometry, vapor generator and evaporator temperatures.

Although optimization is possible by varying the nozzle throat area, this system still presents a mixer and a diffuser with constant geometry. In other words, the shape factors are not optimal for all operating conditions, therefore leading to lower ejector efficiencies. Moreover, the presence of moving parts may compromise system mechanical reliability. To avoid these drawbacks, a multi-ejector pack solution is proposed in this paper for hybrid ejector cooling plants. In these systems, the number of active (differently sized) ejectors is dependent on current operating conditions and determined by a control unit. An accurate design in terms of ejector number and geometry, and a calibrated control strategy is then needed to enable the ejector pack to achieve near optimal performance under variable boundary conditions.

To the best of our knowledge, there are no studies regarding possible control strategies and optimal designs for multi-ejector packs employed in waste heat recovery systems. Dedicated experiments or dynamic simulations under different climatic conditions would be highly useful to investigate system seasonal behavior and performance, especially when compared to conventional refrigerating plants available on the market.

The aim of this work was to compare the performance of different chiller technologies using a thermo-economic analysis with a focus on the seasonal performance of the hybrid multi-ejector cooling system. The paper consists of two main parts: in the first, the sizing process for each component of the hybrid ejector cooling system is described, assuming a specific nominal load and three different climatic zones; the second part presents an analysis of seasonal performance including a parametric analysis to quantify the advantages of using a multi-ejector system by varying the number of ejectors and their geometrical aspects. Furthermore, an optimization analysis in terms of hybrid ejector system design is carried out by proposing three different solutions for achieving different goals such as the minimization of investment costs and the maximization of performance. Additionally, the best choice representing the optimal cost/performance tradeoff is proposed. The proposed system is finally compared to actual chiller technologies (electric and absorption) in terms

of total costs including set-up as well as running costs for different electric energy prices and climatic zones, by assuming the hypothesis of continuous and free availability of the heat source.

2. Description of the Thermodynamic Hybrid Ejector Cycle

A schematic layout of the hybrid ejector cycle is shown in Figure 2a, and the thermodynamic cycle on the T - s diagram of the hybrid ejector cycle is shown in Figure 2b. The description of the thermodynamic cycle can be found in our previous open-access work [11].

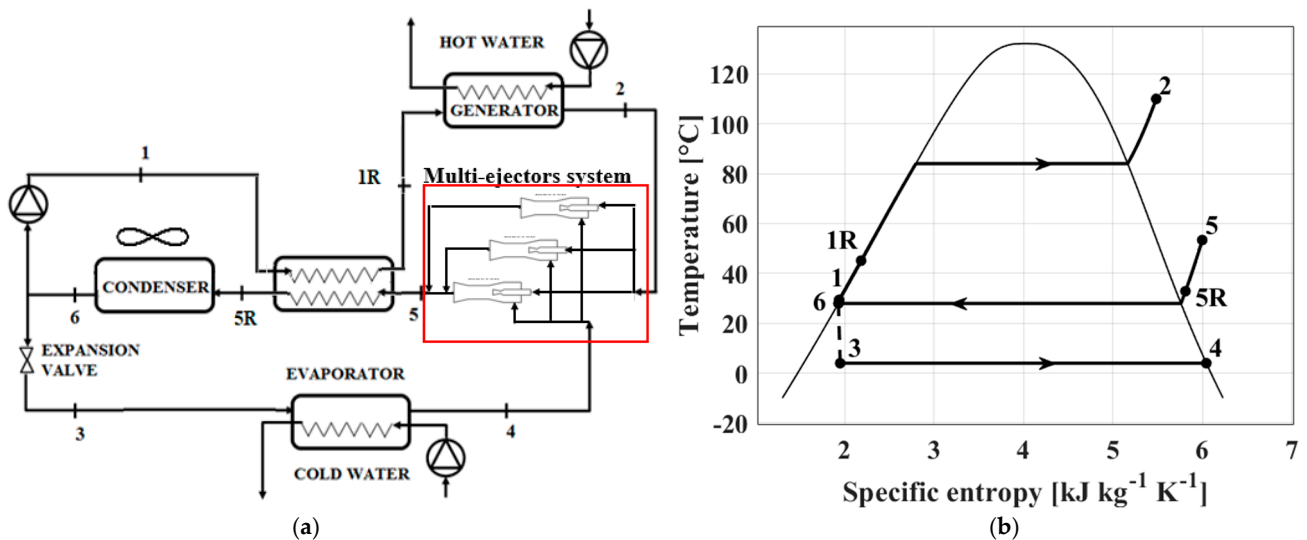


Figure 2. (a) Schematic lay-out of the hybrid ejector cycle proposed in this analysis; (b) Example of an ejector cooling cycle on T - s diagram for the fluid R717.

To evaluate the system performance, two different energy efficiency ratios (EER) can be used: one that considers only the thermal power at the vapor generator as input for the system, and another that considers the electrical power required by the refrigerant pump and auxiliary components.

$$EER_{th} = \frac{\dot{Q}_{ev}}{\dot{Q}_{gv}}; EER_{el} = \frac{\dot{Q}_{ev}}{\dot{W}_p + \dot{W}_{fan}} \quad (1)$$

3. System Modeling

3.1. Ejector Model

To evaluate the maximum ejector performance and the related optimal geometric characteristics, the method presented in Chen et al. [15] was used. This approach was chosen thanks to its relative simplicity and high reliability, having been validated for different refrigerants and operating conditions. The model considers the shock processes inside the ejector and the mixing process occurring at constant pressure, lower than the secondary flow one. The analytical description is simplified by assuming the hypothesis of ideal gas behavior and negligible primary and secondary flow velocities before the ejector inlet section as well as negligible velocity of the mixed flow at the ejector outlet. The model evaluates the best entrainment ratio μ and the related area ratio A_r once the properties at primary and secondary (points 2 and 4, respectively) and the pressure value at the outlet (point 5) are provided.

The entrainment ratio expresses the ratio between the secondary mass flow rate m_{sf} (kg s^{-1}) and the primary mass flow rate m_{pf} (kg s^{-1}). Applying energy and momentum balances and by considering friction losses in terms of isentropic efficiencies in the nozzle

(η_N), in the mixing chamber (η_M) and in the diffuser (η_D), the entrainment ratio can be expressed as Equation (2) [15].

$$\mu = \frac{\dot{m}_{sf}}{\dot{m}_{pf}} = \frac{\sqrt{2} \eta_N (h_2 - h_{7s}) - \sqrt{2} (h_{5s} - h_9) / (\eta_D \eta_M)}{\sqrt{2} (h_{5s} - h_9) / (\eta_D \eta_M) - \sqrt{2} (h_4 - h_8)}; \eta_N = \frac{h_2 - h_7}{h_2 - h_{7s}}; \eta_M = \frac{u_9^2}{u_{9s}^2}; \eta_D = \frac{h_{5s} - h_9}{h_5 - h_9} \quad (2)$$

The ejector cross section design process is carried out by imposing the given efficiencies, and therefore, the system would work with those efficiency values in the nominal conditions. At partial load, we expect that the efficiencies will be affected by a change in operating conditions, but on this point, to the best of our knowledge, there are no available works providing the ejector performance maps or phenomenological models to be implemented. Because the operating conditions are not extremely variable for most of the system operating period, we considered constant values of the efficiencies ($\eta_N = 0.9$, $\eta_M = 0.8$, $\eta_D = 0.9$) for all the simulated points.

The specific enthalpy h_5 can be evaluated by an energy balance on a control volume including the ejector, as in Equation (3).

$$h_5 = \frac{h_2 + \mu h_4}{1 + \mu} \quad (3)$$

The ratio of the constant area of the mixing chamber (A_m) over the throat area (A_t) defines the parameter A_r , expressed according to Chen et al. [15].

$$A_r = \frac{A_m}{A_t} = \frac{p_2 (1 + \mu)^{0.5} (1 + \mu T_4 / T_2)^{0.5} [2 / (k + 1)]^{1 / (k - 1)} [1 - 2 / (k + 1)]^{0.5}}{p_c (p_9 / p_5)^{1 / k} [1 - (p_9 / p_5)^{(k - 1) / k}]^{0.5}} \quad (4)$$

The nozzle throat section A_t can be calculated by assuming choked conditions at the nozzle throat, according to Equation (5) [16] that defines the mass flow rate of the primary flow.

$$\dot{m}_{pf} = \frac{p_2 A_t}{\sqrt{T_2}} \sqrt{\frac{k}{R} \left(\frac{2}{k + 1} \right)^{(k + 1) / (k - 1)}} \sqrt{\eta_N} \quad (5)$$

Finally, the pressure lift Π and the primary-to-outlet ejector pressure ratio β are defined in the following Equation (6):

$$\Pi = \frac{p_5}{p_4} = \frac{p_{co}}{p_{ev}}; \beta = \frac{p_2}{p_5} = \frac{p_{gv}}{p_{co}}; \mu = \frac{\dot{m}_{sf}}{\dot{m}_{pf}} = \frac{\dot{m}_{ev}}{\dot{m}_{gv}} \quad (6)$$

The equations showed above also can be used when the ejector geometry is known and the entrainment ratio at given ejector boundary conditions must be calculated. In this case, the input parameters are the ejector geometry, the thermodynamic state of primary and secondary flows, and the pressure at the ejector outlet.

3.2. Heat Exchanger Surface Evaluation

Proper heat transfer correlations were considered for each heat exchanger to estimate their surface. Regarding the regenerative heat exchanger and the high pressure evaporator, the use of plate heat exchangers is preferable with respect to shell-and-tube heat exchangers thanks to their compactness. Considering the lower pressures, a flooded evaporator was chosen for the cold evaporator, with boiling occurring at the outer surface of the tube bundle, thus avoiding large pressure drops. As regards the condenser, a fin and tube heat exchanger was chosen.

Because of the occurrence of single phase/two phase transitions during heat transfer processes, the overall heat transfer coefficient U ($W m^{-2} K^{-1}$) was appropriately calculated

with dedicated heat transfer prediction methods. The heat transfer equation reported as Equation (7) was applied to each discrete surface dA for any heat exchanger.

$$\delta\dot{Q}(z) = U(z)dA \cdot [T_{hot}(z) - T_{cold}(z)] \quad (7)$$

The overall heat transfer coefficient takes into account both conductive and convective thermal resistances, related to the cold and hot sides of the heat exchanger, as shown in Equations (8) and (9):

$$U = \frac{1}{\frac{1}{\alpha_{ref}} + \frac{\delta}{\kappa_{mat}} + \frac{1}{\alpha_f}} \quad (8)$$

$$\alpha = \frac{Nu \cdot \kappa_{fluid}}{D_h} \quad (9)$$

The detailed list of correlations for the convective heat transfer coefficient for the chosen geometries, including single-phase and two-phase heat transfer can be found in our previous open-access work [11]. The elementary geometric details for each heat exchanger type are defined in the Appendix A.

For the integration of fluid properties, the energy balance was also applied to both cold and hot sides, as expressed in Equations (10) and (11):

$$h_{ref}(z+1) = h_{ref}(z) - \frac{d\dot{Q}}{\dot{m}_{ref}} \quad (10)$$

$$h_f(z+1) = h_f(z) - \frac{d\dot{Q}}{\dot{m}_f} \quad (11)$$

Ideal gas equations were used for the ejector modeling, whereas the remaining thermodynamic and transport properties of refrigerant and secondary fluids were evaluated with Refprop 9.1, developed by NIST [17].

3.3. Other Components

In order to evaluate the real operating functioning of the working fluid pump, the global efficiency was evaluated as a function of the differential pressure, as shown in Figure 3. Equation (12) was used to estimate the pump efficiency according to the experimental results given by Declay [18]. This function was calibrated for a compression ratio typical of ORC cycles, which are somewhat higher than those exploited for the present analysis.

$$\eta_{gl} = -2.6 \cdot 10^{-4} \Delta p^2 + 0.025 \Delta p + 0.002 \quad (12)$$

The electric power required by the fans of the condenser was calculated with Equation (13), where the fan efficiency η_{fan} is evaluated by the fan map performance collected by a market analysis.

$$\dot{W}_{fan} = \frac{\Delta p_{air} \cdot \dot{V}_{air}}{\eta_{fan}} \quad (13)$$

3.4. Working Fluids

According to the work of Varga et al. [19] and to the results of a preliminary thermo-economic analysis described in our previous publication [11], hybrid ejector cooling systems employing ammonia as working fluid represent the best performing solution with respect to hydrocarbons and HFOs, thanks to the high latent heat and advantageous thermodynamic and transport properties for boiling heat transfer. Moreover, the ammonia's higher saturation pressures might lead to compact plate heat exchangers, thus reducing set-up costs. Therefore, ammonia was considered as the working fluid in the current analysis.

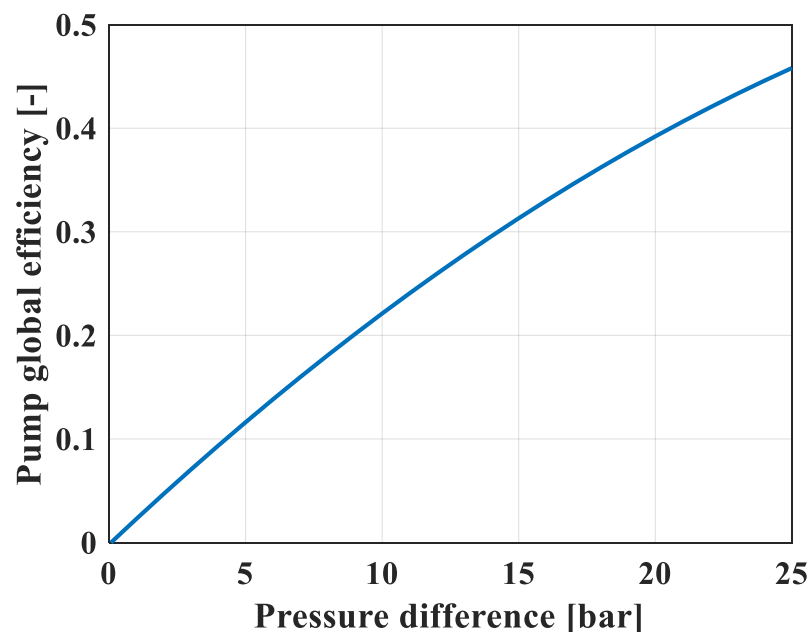


Figure 3. Pump global efficiency as function of pressure difference [18].

4. Component Sizing

The first part of the current analysis proposes the sizing of each component of the hybrid ejector cooling cycle (heat exchangers, refrigerant pump and ejector) for three different climatic zones by assuming for all zones the same value of nominal cooling load. In the sizing process, a single ejector with fixed geometry was considered; the design and the use of a multi-ejector pack instead of a single ejector will be described in the following sections. Since the ambient temperature has a relevant influence on the system performance, the condenser design process is a sensitive issue. Hence, in order to evaluate its geometry, a detailed analysis was carried out by varying different geometric parameters such as tube step, fin thickness, number of tubes and number of rows. For each climatic zone, different solutions were selected in order to minimize the investment costs or to maximize the system performance. Additionally, among all the feasible solutions, an optimal configuration was considered. The optimization processes for the vapor generator and evaporator are not described in the current paper. In particular, the plate heat exchanger (vapor generator) was characterized by low purchase costs with respect to the other devices, such as the fin and tube heat exchanger (condenser) and the flooded evaporator. Furthermore, the operating costs related to the water loop circulating pump were not considered in this analysis. As regards the flooded evaporator, the refrigerant pressure drops were negligible and the chosen geometry was already optimized by calculating the required number of tubes to obtain a water Reynolds number at least equal to 2×10^4 , thus guaranteeing optimized heat transfer performance. According to these considerations, only the optimization of the condenser is described, and its influence on the total investment costs and system performance is discussed in detail.

4.1. Algorithm

The solution algorithm was implemented in Matlab environment. By knowing the pinch point value and the cold water temperature, the low-pressure evaporation temperature was directly calculated, whereas the high-pressure evaporator and the condenser saturated conditions were obtained by an iterative process searching for the desired pinch point value. Firstly, the condensation and high temperature evaporator pressures were predicted, thus obtaining the complete thermodynamic cycle. Then, the pinch point value (that occurs at saturated vapor for the condenser and instead in liquid condition for the high-temperature evaporator) was calculated, thus adjusting the predicted pressure values

accordingly, up to the convergence in the design temperature difference. For instance, if the pinch point value was higher than the design value, the condenser/evaporator pressure was accordingly decreased/increased. Once the thermodynamic properties were defined, the heat exchanger models were applied to evaluate the heat transfer surfaces.

The following steps are included in the heat exchanger solution procedure:

1. The thermodynamic and geometric parameters are fixed as input for the model.
2. The working fluid temperatures at the inlet ($z = 1$) of generator, condenser and evaporator are set equal to the temperature values in points 2, 5 and 4, respectively.
3. Proper heat transfer prediction methods [11] and Equations (8) and (9) are used to calculate the heat transfer coefficient U for each elementary volume.
4. The elementary heat power is obtained from Equation (7).
5. The specific enthalpy (and temperature) of the following ($z + 1$) integration step are calculated with energy balances from Equations (10) and (11).
6. By using the thermodynamic properties evaluated in the previous step, the procedure (from step 3 to 5) is reiterated until the overall heat exchanger surface is able to handle the required heat power.

At this point, the heat transfer surface A is known for all heat exchangers in any geometric configuration and at any boundary condition. The fixed and unknown geometric parameters for all the heat exchangers are given in the Appendix A.

4.2. Cost Functions

The investment costs were calculated by using the set-up cost of any component by using cost correlations listed and commented in detail in our previous open-access work [11]. Toxicity and flammability issues related to the use of ammonia as working fluid were considered by using a corrective enhancement factor of 1.30. The costs related to the waste heat utilization system (investment and operating costs) were not considered in this analysis.

4.3. Operating Conditions and Weather Data

The sizing of the hybrid ejector cycle was performed by considering a nominal cooling load of 20 kW supplied by hot water at 120 °C at the vapor generator inlet. In the current analysis, a continuous and freely available hot source was considered. The data used are listed in Table 1. To highlight the effects of different values of the external ambient temperature, three climatic zones (Milan, Madrid, Athens) were considered in the design process. The sizing of the components was carried out by assuming the occurrence of a nominal cooling load when the external ambient temperature was equal to the maximum value, according to weather data obtained by TRNSYS software libraries [20]. The set-point indoor temperature was set to 26.0 °C. The maximum temperature values for each climatic zone are reported in Table 2.

Table 1. Specification of the boundary conditions used for the sizing process.

Parameters	Value	Parameters	Value
Nominal cooling load [kW]	20	Water temperature at the evaporator (inlet/outlet) [°C]	12/7
Working fluid temperature at vapor generator outlet [°C]	110	Quality at evaporator outlet	1.0
Water temperature at the vapor generator (inlet/outlet) [°C]	120/80	Regenerative heat exchanger efficiency	0.90
Air temperature difference at the condenser [K]	5	Pinch points for the heat exchangers [K]	3
Quality at condenser outlet	0.0	Set point indoor temperature [°C]	26.0

Table 2. Maximum external ambient temperatures for each climatic zone.

Climatic Zone	$T_{amb,max}$ [°C]
Milan	32.50
Madrid	36.70
Athens	37.45

4.4. Results

The geometric combinations investigated in the condenser sizing process, listed in detail in the Appendix A, led to multiple solutions in terms of total investment costs (IC) and total electric load. Figure 4 shows all feasible solutions for each investigated climatic zone. It is evident that a Pareto front existed on the plane electric load/set-up costs: to quantify the effects of different sizing criteria on the seasonal performance analysis, the two extreme solutions were considered for each climatic zone. Solution A represents the configuration characterized by the minimum set-up cost and solution B the minimum energy consumption configuration. It is worth noting that solutions A and B do not represent practical options, but are able to give information about all the intermediate ones. Furthermore, an optimal solution C, characterized by the minimum distance with respect to the utopia point, was also considered in the seasonal performance analysis. The choice of sizing criteria has great influence on the system performance/costs: when considering Milan as climatic zone, passing from solution A to C, a percentage increase in the total IC equal to 11.8% led to a wide reduction (−77%) in terms of energy consumption, passing from 20.67 kW to 4.73 kW. Instead, passing from solution C to B, an increase in IC equal to 45.4% reduced the required electric load from 4.73 kW to 1.20 kW. More details on the sizing results are reported in Table 3.

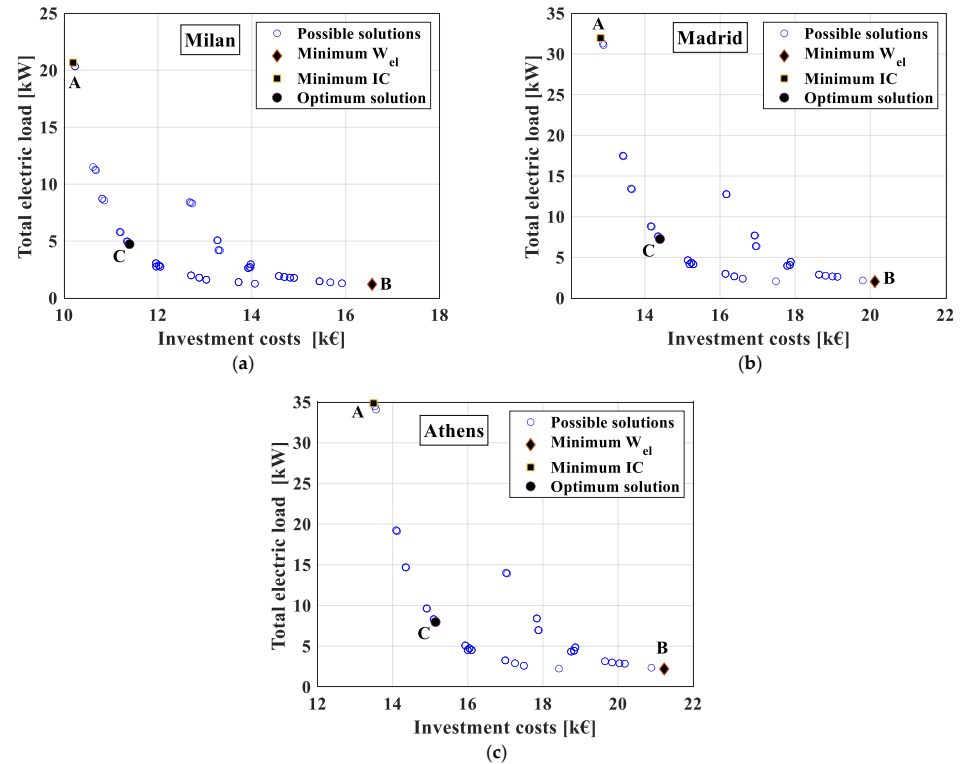


Figure 4. Total electric load of all feasible hybrid ejector configurations as function of set-up costs for (a) Milan, (b) Madrid, (c) Athens. The distinctive points represent the arrangement characterized by the minimum costs A, the one with minimum electric load B and the optimal one C identified by the best compromise between performance and costs.

Table 3. Sizing results.

Climatic Zone	Solution	T_{gv} [°C]	T_{co} [°C]	T_{ev} [°C]	D_t [mm]	$D_{N,out}$ [mm]	D_m [mm]	A_{gv} [m ²]	A_{co} [m ²]	A_{ev} [m ²]	A_{rhe} [m ²]	μ [-]	EER_{el} [-]	IC [k€]
Milan	A	83.0	40.3	4.0	3.71	4.82	6.90	7.20	152.56	1.33	0.33	0.184	0.97	10.194
	B	83.0	40.3	4.0	3.71	4.82	6.90	7.20	407.29	1.33	0.33	0.184	16.61	16.563
	C	83.0	40.3	4.0	3.71	4.82	6.90	7.20	200.56	1.33	0.33	0.184	4.23	11.394
Madrid	A	82.2	44.4	4.0	4.55	5.91	7.78	10.48	202.11	1.33	0.47	0.127	0.63	12.819
	B	82.2	44.4	4.0	4.55	5.91	7.78	10.48	494.23	1.33	0.47	0.127	9.87	20.122
	C	82.2	44.4	4.0	4.55	5.91	7.78	10.48	265.32	1.33	0.47	0.127	2.76	14.399
Athens	A	82.0	45.2	4.0	4.75	6.17	8.00	11.30	215.25	1.33	0.50	0.118	0.57	13.491
	B	82.0	45.2	4.0	4.75	6.17	8.00	11.30	524.85	1.33	0.50	0.118	9.09	21.231
	C	82.0	45.2	4.0	4.75	6.17	8.00	11.30	281.31	1.33	0.50	0.118	2.51	15.142

T_{gv} = vapor generator temperature; T_{co} = condensing temperature; T_{ev} = evaporating temperature; D_t = motive nozzle throat section diameter; $D_{N,out}$ = motive nozzle outlet section diameter; D_m = mixing section diameter; A_{gv} = vapor generator heat transfer surface; A_{co} = condenser heat transfer surface; A_{ev} = evaporator heat transfer surface; A_{rhe} = regenerative heat exchanger heat transfer surface; μ = entrainment ratio; EER_{el} = electric EER defined in Equation (1); IC = investment costs.

5. Seasonal Performance

The second part of the current analysis investigated the performance of the hybrid ejector cooling system during the summer season, once the system had been sized in the previous section. The use of a multi-ejector system instead of a single ejector was considered, since ejectors with fixed geometry are unable to provide acceptable performance when varying the operating conditions (especially external ambient temperature). The specifications for number of ejectors and geometric aspects are described in the following section.

The seasonal performance was evaluated by the seasonal energy efficiency ratio $SEER_{el}$, which considers as input the electric energy required by the refrigerant pump $E_{el,p}$ (kWh) and the condenser fans $E_{el,fan}$ (kWh), as defined in Equation (14).

$$SEER_{el} = \frac{\sum Q_{ev}}{\sum (E_{el,p} + E_{el,fan})} \quad (14)$$

5.1. Multi-Ejector System: Configurations and Control Strategy

In addition to the configuration with one ejector, solutions with 2 to 9 ejectors were investigated and different criteria for multi-ejector sizing were considered in order to obtain the optimal multi-ejector configuration for each climatic zone. The ratio of each ejector cross section (nozzle throat, nozzle outlet, mixing section) between two subsequent ejectors assumed the following values: 0% (ejector with the same size), 20% (the cross section of ejector 2 is 20% larger than that of ejector 1), 40%, and 80%. In the subsequent sensitivity analysis, we simulated all possible cases (from 1 to 9 ejectors with all geometric scale values). It is worth noting that the sum of the cross sections of all the ejectors was always equal to the cross section of the nominal size ejector. The specifications of the investigated multi-ejector packs are listed in Table 4.

Table 4. Multi-ejector pack specifications.

Parameters	Value
Number of ejectors [#]	1–9
Multi-ejector geometric scale ϕ_{ej}	0; 20; 40; 80

Differently from the case with one ejector, various configurations of the multi-ejector system are able to satisfy the cooling load required by the user. Such a condition occurs when the secondary mass flow rate of the multi-ejector is higher than the evaporator mass flow rate ($m_s > m_{ev}$). The employed multi-ejector control strategy is reported in Figure 5 showing the trend of the secondary mass flow rate as a function of condensing temperature for different values of vapor generator temperature; meanwhile, the dotted line represents

the evaporator mass flow rate. A multi-ejector configuration with 4 ejectors having the same size was assumed. As can be seen from Figure 5, there exists a minimum number of ejectors able to satisfy the cooling load (2 active ejectors); this condition represents the oversized configuration of the multi-ejector because the secondary mass flow rate of the multi-ejector pack m_s is higher than the evaporator mass flow rate m_{ev} . Among the possible solutions in terms of T_{gv}/T_{co} , the one characterized by the higher value of the entrainment ratio was considered according to the heat transfer matching in the heat exchangers.

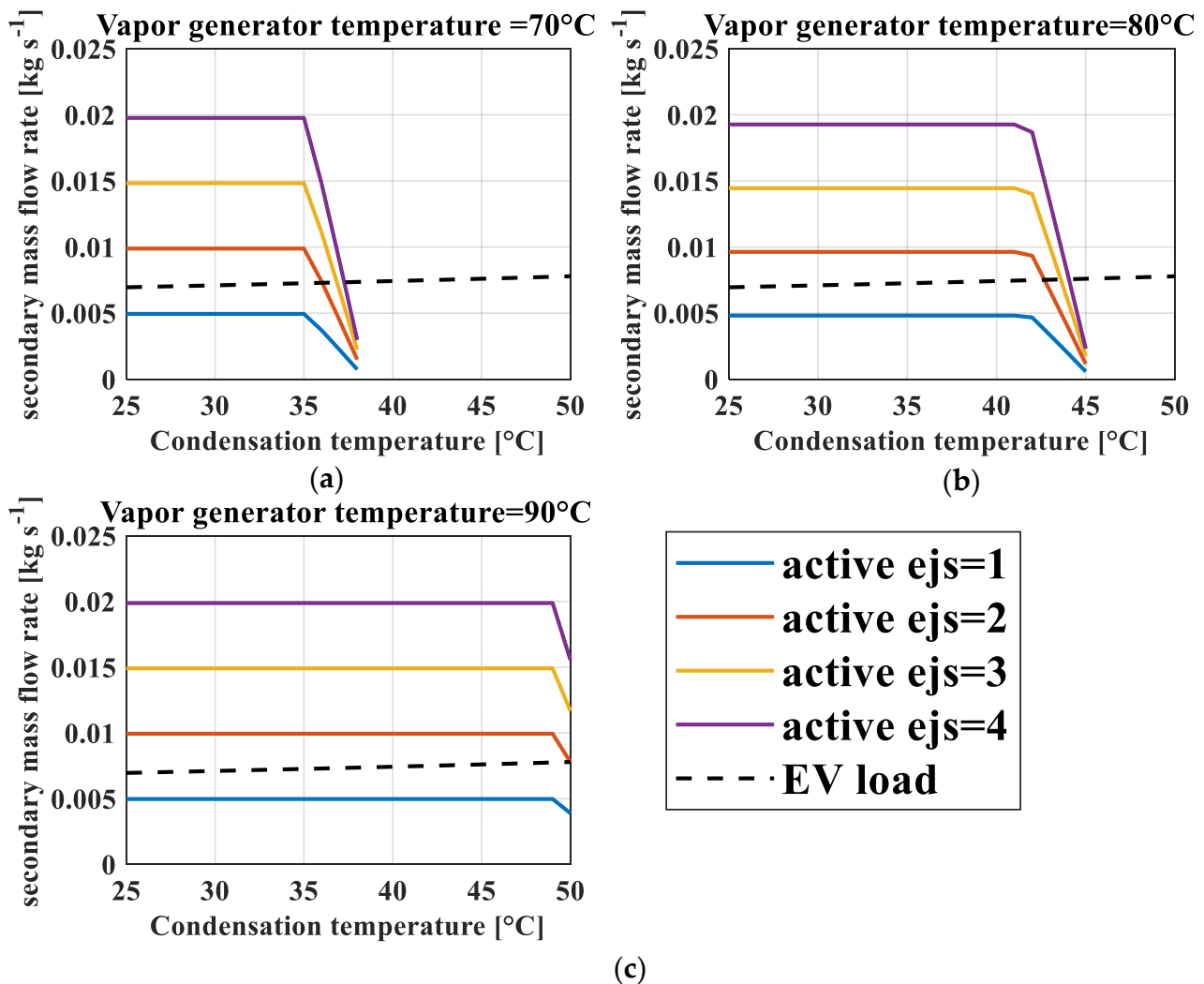


Figure 5. Example of multi-ejector control strategy assuming four ejectors with the same size at (a) $T_{gv} = 70\text{ }^{\circ}\text{C}$, (b) $T_{gv} = 80\text{ }^{\circ}\text{C}$, (c) $T_{gv} = 90\text{ }^{\circ}\text{C}$.

In order to balance the required cooling load, the multi-ejector system will work both with the oversized configuration ($m_s > m_{ev}$) and with the condition immediately preceding it. The latter, called under-sized configuration ($m_s < m_{ev}$), was characterized by 1 active ejector, according to the blue line in Figure 5. The operating time ϑ of the oversized configuration was evaluated with Equation (15).

$$\vartheta = \frac{\dot{Q}_{user} - \dot{Q}_{ev}^{ej,under}}{\dot{Q}_{ev}^{ej,over} - \dot{Q}_{ev}^{ej,under}} \quad (15)$$

Once the operating time ϑ was known, the total electric load E_{el} [kWh] could be evaluated with Equation (16).

$$E_{el} = \dot{W}_{el}^{ej,over} \cdot \vartheta + \dot{W}_{el}^{ej,under} \cdot (1 - \vartheta) \quad (16)$$

Different multi-ejector control strategies could be considered; however, it was preferred that continuous operation of the system be guaranteed by avoiding frequent power cycling that would lead to a decrease in system performance. Employing this control strategy, on/off regimes occurred only when the oversized multi-ejector configuration consisted of 1 active ejector.

5.2. Algorithm

The solution algorithm was developed and implemented in Matlab environment. Once the multi-ejector configuration, the heat exchangers geometry and the working fluid were fixed, the seasonal performance could be evaluated by considering the variation in external ambient temperature, and hence the cooling load required by the final user, according to the summer cooling season as described in the following section. The hot water temperature at the vapor generator and its variation across the heat exchanger were input parameters, as well as the external air temperature variation across the condenser and the chilled water temperature. The hybrid ejector seasonal performance was evaluated for each sizing configuration (A, B, C). Due to the unknown pinch-point temperatures, the saturation temperatures were obtained with an iterative process.

The solution procedure described here was performed for each operating hour of the cooling season characterized by different climate conditions. The following steps were included in the solving procedure:

1. The multi-ejector configuration, the working fluid, secondary fluid inlet/outlet temperatures and heat exchanger geometry are fixed as inputs for the algorithm;
2. The ambient temperature and the cooling load at the evaporator are fixed and obtained from the weather data file;
3. The evaporation temperature is assumed: the temperature profiles are obtained and the overall heat transfer coefficient U can be evaluated by the logarithmic mean temperature difference. This value is then compared to the one obtained by the heat transfer correlations. The evaporation temperature is adjusted until the matching between the heat exchanger project equation and the heat transfer correlations is obtained;
4. Once the cooling load is defined, the undersized and oversized multi-ejector configurations can be selected as described in the previous section;
5. The first values of the vapor generator and condenser saturation temperatures are fixed, and the thermodynamic cycle is evaluated;
6. The ejector boundary conditions are known, and the entrainment ratio is obtained with the ejector model. Hence, the mass flow rates and the thermal powers can be evaluated;
7. The condenser is numerically solved as described before, and the heat transfer surface is calculated and compared to the one obtained by the design process. The condenser saturation temperature is adjusted up to the numerical convergence (with a fixed tolerance of 0.05) by repeating steps 5, 6 and 7;
8. With the correct condensation temperature, the vapor generator is integrated in order to evaluate its heat transfer surface. The vapor generator saturation temperature is then adjusted by repeating steps 5, 6, 7 and 8 up to the numerical convergence (keeping the same tolerance of step 7) between heat transfer surfaces.
9. The steps from 5 to 8 are performed for each multi-ejector configuration according step 4.
10. The thermodynamic cycle and the thermal and electrical powers are known: the oversized multi-ejector configuration operating time is evaluated with Equation (15)

and the electrical load required by the fans and the refrigerant pump are calculated with Equation (16). Finally, the seasonal performance indicator $SEER_{el}$ is evaluated with Equation (14).

5.3. Operating Conditions and Weather Data

The data used to evaluate the seasonal performance of the hybrid ejector cooling cycle are listed in Table 5 and include both thermodynamic and geometric parameters.

Table 5. Specifications of the boundary conditions used for the seasonal simulation process.

Parameters	Value	Parameters	Value
Working fluid temperature at vapor generator outlet [°C]	110	Quality at condenser outlet	0.0
Water temperature at the vapor generator (inlet/outlet) [°C]	120/80	Quality at evaporator outlet	1.0
Air temperature difference at the condenser [K]	5	Heat exchanger geometry	from the sizing procedure
Water temperature at the evaporator (inlet/outlet) [°C]	12/7	Ejector geometry	from the sizing procedure

Figure 6b,d,f show the temperature profiles of the investigated climatic zones [20]. The building global conductance UA [kW/K] is given by Equation (17):

$$\dot{Q}_{nom} = (UA)_{build} \cdot [T_{amb,max} - T_{user}] \quad (17)$$

Once the building global conductance is evaluated for each investigated climatic zone, the related cooling profile can be obtained. In particular, the cooling system runs when the indoor temperature is higher than the set-point indoor temperature (plus a tolerance of 0.5 °C). Figure 6a,c,e show the operating time and the probability density function for the cooling profile for each climatic zone.

5.4. Results

Firstly, the influence of the multi-ejector configuration on the system performance was investigated in order to find the number of ejectors and their geometry maximizing the seasonal performance for each climatic zone. Once the optimal multi-ejector configuration was identified, it was used for a thermo-economic comparison by considering electrical and absorption chillers as conventional cooling technologies.

5.4.1. Multi-Ejector System Optimization

Figure 7a–c show the influence of the number of ejectors on seasonal performance, for each investigated climatic zone and ejector area ratio. The use of a multi-ejector system increases the system performance significantly: when increasing the ejector number from 1 to 2 with an area ratio of +80%, the $SEER_{el}$ increased 47.8%, 79.3% and 89.9% for Milan, Madrid and Athens respectively (solution C). This result highlights the major benefits that could be obtained with a multi-ejector system instead of a single ejector with fixed geometry. Furthermore, the warmer the climate, greater the advantages of multiple ejectors. As regards the system optimization, the trends in Figure 7a–c show that multi-ejector packs with 3 or 4 ejectors deliver the maximum in terms of $SEER_{el}$ regardless of the climate zone or multi-ejector geometry (except for ejectors of the same size, $\phi_{ej} = 0\%$). Further increasing the number of ejectors leads to minor performance enhancements but could pose technical issues in terms of multi-ejector system control. It is worth noting that, by increasing the number of ejectors, the $SEER_{el}$ tends to an asymptotic value; in this case, there was no influence of the ejectors area ratio.

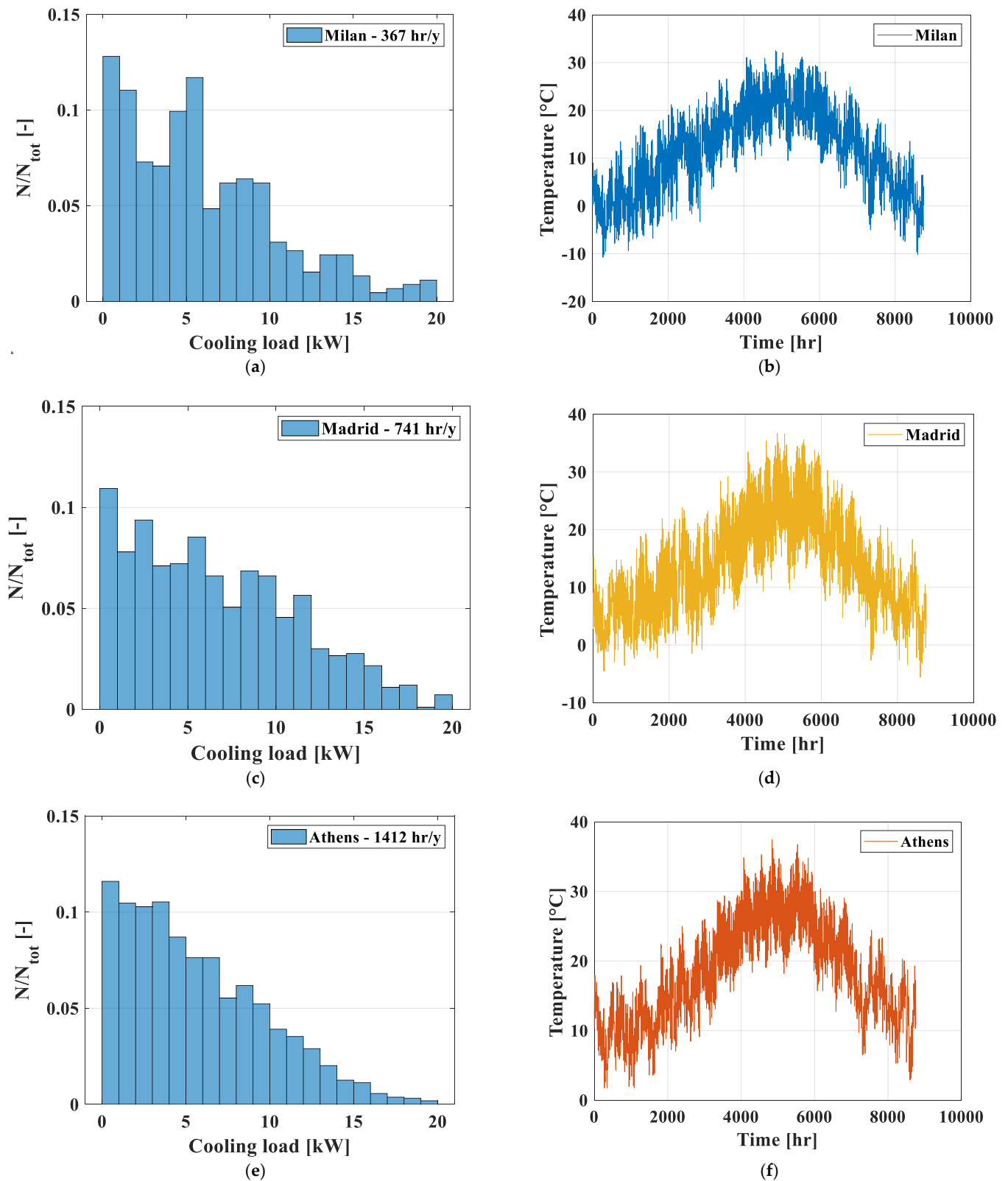


Figure 6. Cooling load profile and seasonal hourly temperature profile for Milan (a,b), Madrid (c,d), Athens (e,f).

5.4.2. Thermo-Economic Comparison with the Current Technology

The seasonal performances were compared to conventional cooling systems, represented by electrical chillers and heat-driven absorption chillers. Following the outcomes

of the preceding paragraph, this analysis was carried out by considering 3 ejectors for the Milan climate ($\phi_{ej} = +20\%$), and 4 ejectors for the cases of Madrid and Athens ($\phi_{ej} = +80\%$). Typical seasonal performance of electrical chillers is reported in [21]; in particular, a $SEER_{el}$ of 4.0 could be obtained when considering Milan as the climatic zone. An air-cooled absorption system was considered, and the $SEER$ was evaluated by treating electrical load as energy input. A $SEER_{el}$ of 6.5 could be obtained in a climatic zone similar to that of Milan, as shown in [22]. The influence of different ambient temperature values on the $SEER_{el}$ of the mentioned technologies was evaluated by considering constant the second law EER and by varying the reversible EER as a function of external ambient temperature. Figure 8 shows the comparison between the ejector cycles (with different sizing criteria) and electrical and absorption chillers. In order to take into account market variation, a tolerance range of $\pm 20\%$ on the seasonal performance was applied. When considering the optimal solution C, the hybrid ejector cooling cycle was characterized by higher performances than the reference technologies, especially in a moderate climatic zone such as Milan, where the $SEER_{el}$ of the ejector cooling cycle was 3.3 and 2.1 times higher than that of the electrical and absorption chillers, respectively. Higher values of ambient temperature significantly decreased the performance of the ejector cycle, from 13.36 to 8.1 (Madrid) and 7.8 (Athens). Furthermore, the difference between ejector cycle and conventional chillers was smaller in the warmer climatic zones, due to the fact that a higher external ambient temperature leads to higher penalizations for the hybrid ejector cycle.

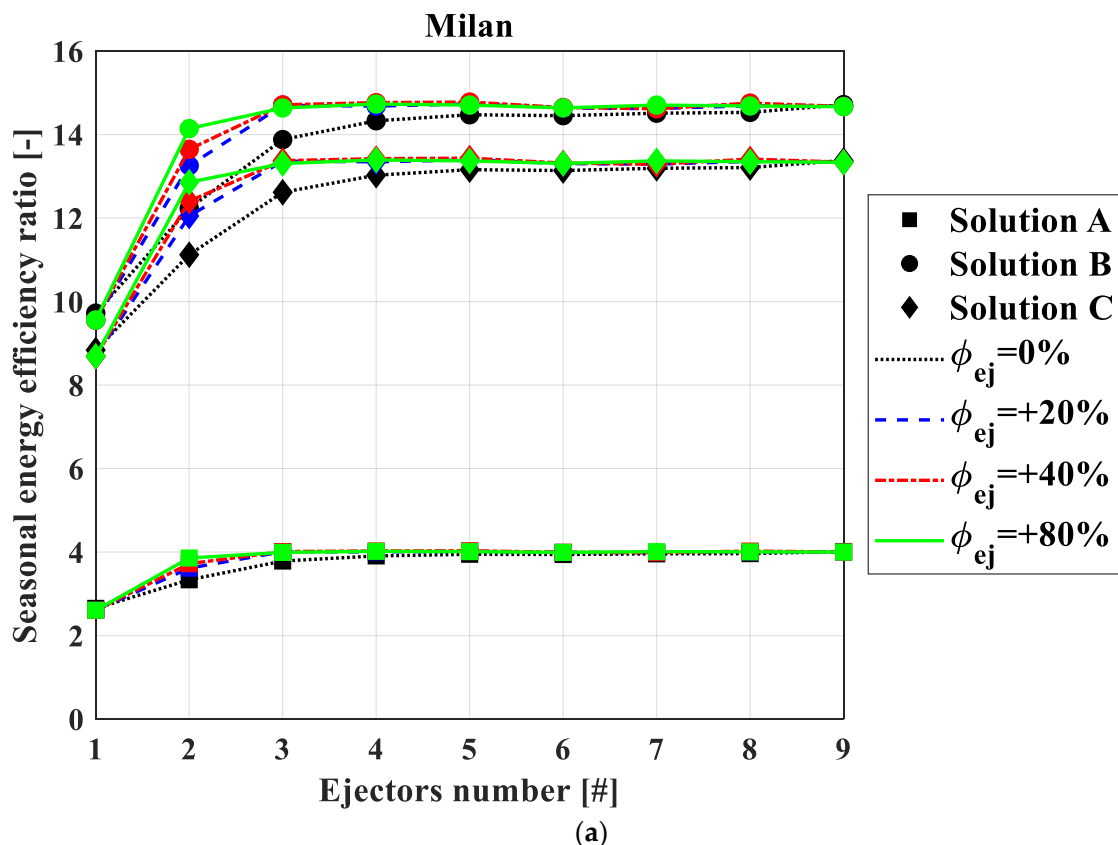


Figure 7. Cont.

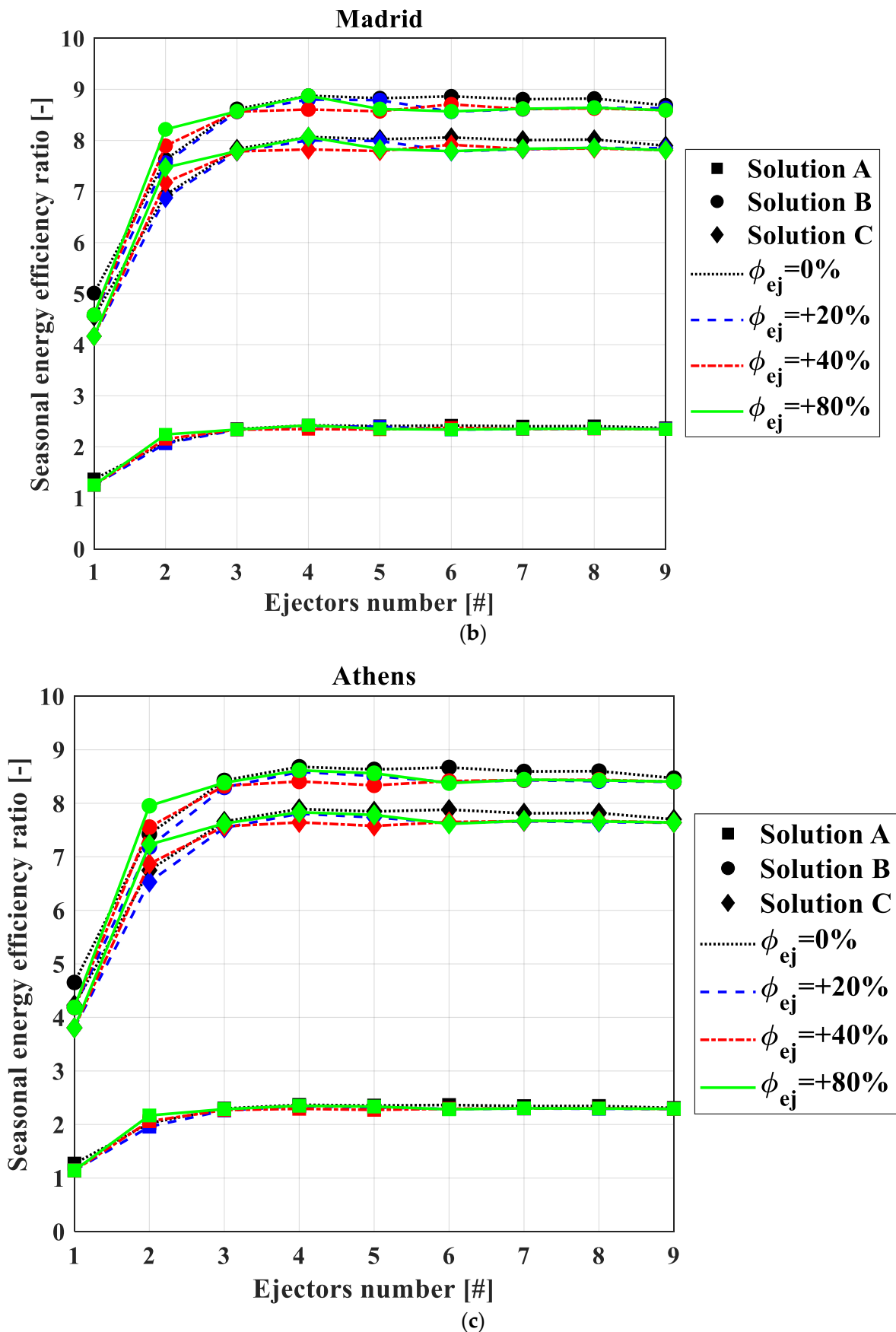


Figure 7. Seasonal performance as function of number of ejectors for (a) Milan, (b) Madrid, (c) Athens and multi-ejector configuration.

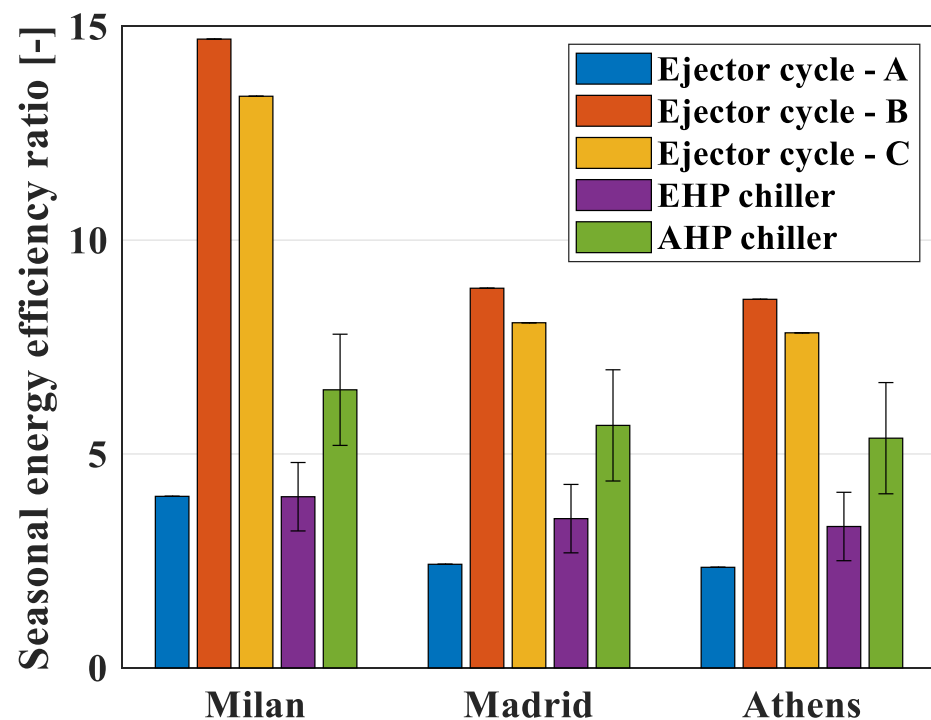


Figure 8. Seasonal performance comparison between hybrid ejector cycle and current technology.

In order to give a complete scenario, an economic analysis was proposed by considering both the investment and running costs. The set-up costs for the hybrid ejector cycle were obtained by considering each component as previously described, whereas the investment costs for electrical and absorption chillers were evaluated from a market analysis perspective [23], as detailed in Table 6. The running costs were evaluated with Equation (18): a lifetime of 20 years and three different values for the electricity-specific price (0.10, 0.30, 0.50 €/kWh) were considered.

$$RC_{lifetime} = \frac{Q_{user}}{SEER_{el}} \cdot c_{el} \cdot \theta_{lifetime} \quad (18)$$

Table 6. Investment costs.

Climatic Zone	Ejector Cycle Solution A	Ejector Cycle Solution B	Ejector Cycle Solution C	EHP Chiller	AHP Chiller
Milan	10.194 €	16.563 €	1.394 €	12.002 €	19.239 €
Madrid	12.819 €	20.122 €	14.399 €	13.202 €	21.163 €
Athens	13.491 €	21.231 €	15.142 €	14.402 €	23.087 €

Finally, total costs could be evaluated with Equation (19):

$$TC_{lifetime} = IC + RC_{lifetime} \quad (19)$$

The numerical details of the simulated cases are listed in Table 7. The table only considers electrical chillers as reference technology because absorption chillers do not represent the most convenient solution in any of the simulated conditions.

Table 7. Economic life of a hybrid ejector cycle with respect to an electric chiller.

Climatic Zone	Convenience Lifetime [Years]		
Hybrid Ejector Solution			
Milan	$c_{el} = 0.10 \text{ €/kWh}_{el}$	$c_{el} = 0.30 \text{ €/kWh}_{el}$	$c_{el} = 0.50 \text{ €/kWh}_{el}$
A—Minimum costs	always	always	always
B—Minimum electric load	never	never	>18.1
C—Optimum	always	always	always
Madrid	$c_{el} = 0.10 \text{ €/kWh}_{el}$	$c_{el} = 0.30 \text{ €/kWh}_{el}$	$c_{el} = 0.50 \text{ €/kWh}_{el}$
A—Minimum costs	<3.3	<1.1	<0.7
B—Minimum electric load	never	never	never
C—Optimum	never	>7.1	>4.3
Athens	$c_{el} = 0.10 \text{ €/kWh}_{el}$	$c_{el} = 0.30 \text{ €/kWh}_{el}$	$c_{el} = 0.50 \text{ €/kWh}_{el}$
A—Minimum costs	<4.2	<1.4	<0.8
B—Minimum electric load	never	never	>15.3
C—Optimum	>9.5	>3.2	>1.9

If the ejector system is designed with an emphasis on performance, as in solution B, the ejector cooling chiller does not represent a practical solution because of its high set-up costs, which lead to an unacceptable break-even time, equal to 18.1 and 15.3 years in Milan and Athens, respectively. Solution A (characterized by lower investment cost but lower performance) would always be advantageous in Milan due to low set-up cost and low external ambient temperature, leading to a reduction in system performance that is not excessive. By contrast, higher running costs in warmer climates imply an impracticable economic life for multi-ejector cooling systems (up to 3.3 and 4.2 years in Madrid and Athens, respectively, when an electricity unit price of 0.10 €/kWh is considered). Higher electricity unit prices reduce the maximum economic life. The potentially optimal solution C was able to match costs and performance and seemed consistently advantageous in moderate climatic zones such as Milan, whereas in warmer climates, the hybrid ejector cooling systems were more beneficial compared to EHP chillers after an acceptable economic life (after 7.1 years in Madrid with 0.30 €/kWh electricity unit price, and after 9.5 years in Athens with 0.10 €/kWh electricity unit price). Of course, scenarios with higher electricity costs make ejector cooling systems more and more economically viable compared to electrically driven technologies with reduced economic lifetimes.

In addition to a comparison between hybrid ejector systems and actual chiller technologies, a specific design solution for an ejector system could be preferred at a fixed electric energy unit price. Figures 9–11 show the total costs as a function of the lifetime by comparing the optimal ejector cooling cycle solution with the reference chiller technologies (electrical and absorption) for three different electricity unit prices. Each figure refers to a specific climatic zone. For a low expected economic life, solution A was the most convenient due to its low set-up cost regardless of climatic zone; meanwhile, the increase in expected economic life made solution C the cheaper hybrid ejector sizing configuration, depending on the electric energy unit price. When considering Milan, solution A was the most convenient throughout its economic lifetime for a $c_{el} = 0.10 \text{ €/kWh}_{el}$, but if the electricity price were 0.50 €/kWh_{el}, solution C would be preferred after an economic lifetime of about 5 years. In Madrid, the lifetime value after which solution C is cheaper than solution A varied from 9.3 to 2 years, when the electric energy unit price trended from 0.50 to 0.10 €/kWh_{el}. However, if Athens was considered, lower lifetime threshold values resulted, trending from 5.7 to 1.2 years for an electricity price range of 0.50 and 0.10 €/kWh_{el}, respectively.

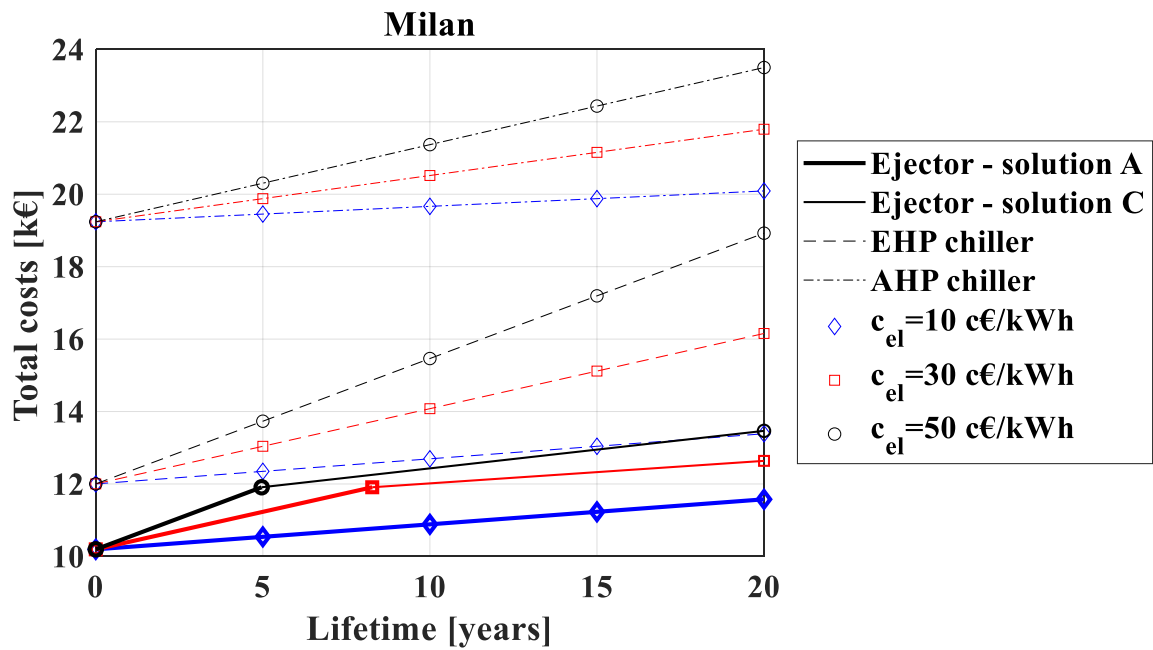


Figure 9. Total costs as function of economic lifetime and electric energy unit price for Milan climatic zone, and comparison between hybrid ejector cycle and current technology.

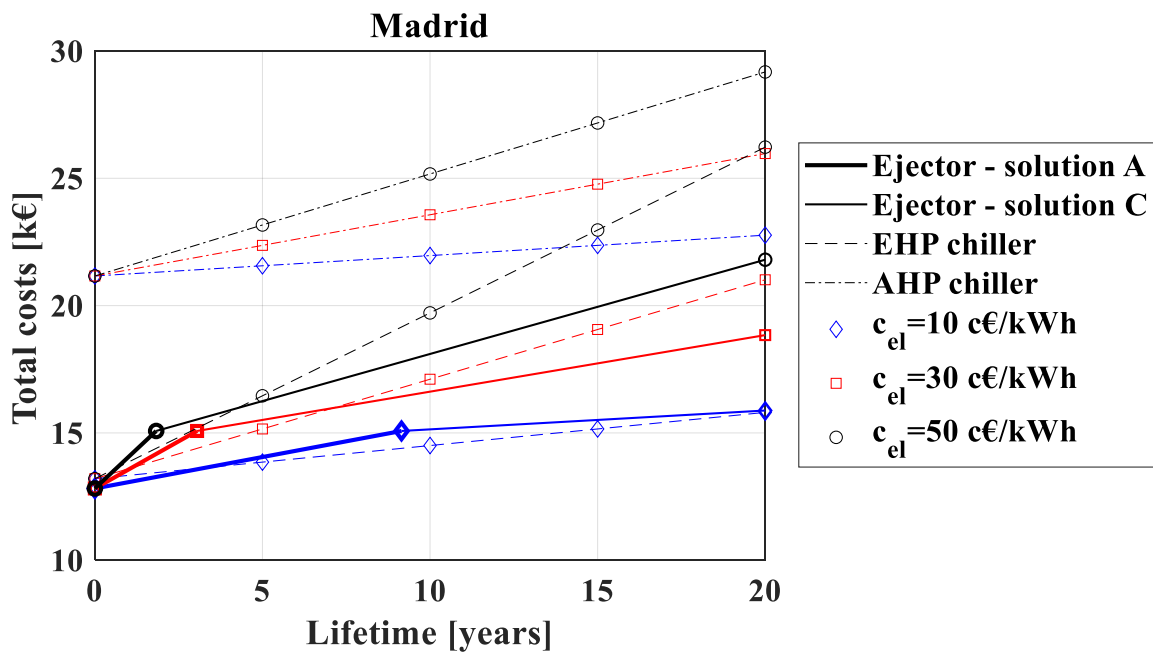


Figure 10. Total costs as function of economic lifetime and electric energy unit price for Madrid climatic zone, and comparison between hybrid ejector cycle and current technology.

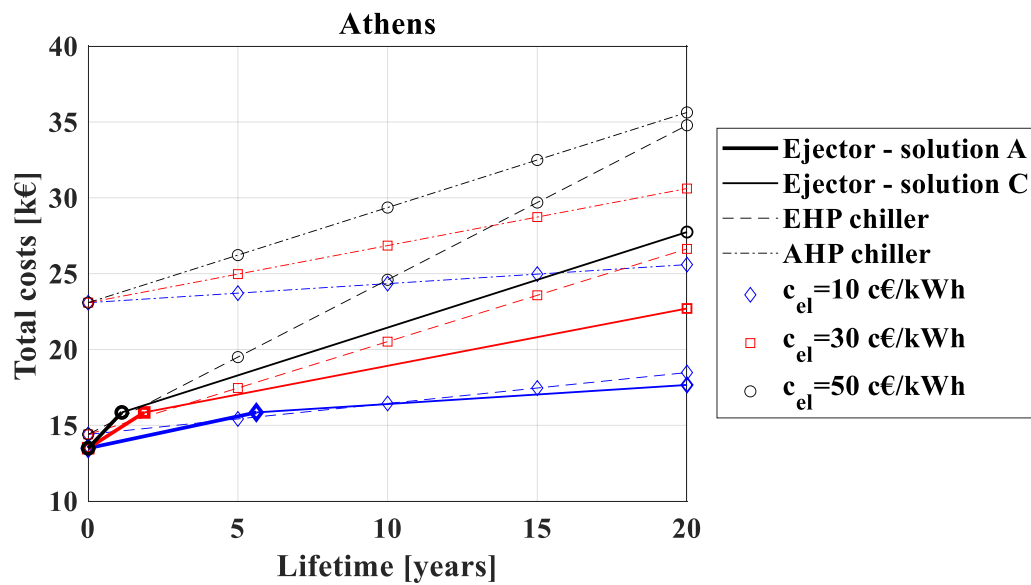


Figure 11. Total costs as function of economic lifetime and electric energy unit price for Athens climatic zone, and comparison between hybrid ejector cycle and current technology.

6. Conclusions

A thermo-economic analysis of a heat-driven hybrid ejector chiller for air conditioning purposes was performed in this paper for the case of a free and continuously available thermal source. The seasonal performance and total costs during a summer season were evaluated for three different climatic zones and different electric energy-specific prices in order to perform a comparison between the hybrid ejector cooling cycle and chiller technologies actually available on the market. The analysis was performed by considering different plant configurations of the ejector cycle: configuration A, minimizing the investment costs; configuration B, maximizing system performance EER_{el} , and configuration C as a tradeoff solution. The main outcomes of this study may be summarized as follows:

- The use of a multi-ejector system instead of a single fixed-geometry ejector enables the system to run at partial load without penalizing seasonal performance. Climatically warmer zones gain major benefits by using multi-ejector packs, with an 89.9% increase in the $SEER_{el}$ in Athens when shifting from 1 to 2 ejectors.
- Regardless of the climatic zone and the multi-ejector geometric scale, except $\phi_{ej} = 0\%$, maximum seasonal performance could be obtained with a multi-ejector system of 3 or 4 ejectors.
- The hybrid ejector cooling cycle is characterized by higher seasonal performances than those of the reference technologies, especially in moderate climatic zones such as Milan, where the $SEER_{el}$ of the ejector cooling cycle is 3.3 and 2.1 times higher than that of electrical and absorption chillers, respectively. All three chiller technologies are characterized by lower performance in warmer climatic zones but the penalty due to higher ambient temperatures is stronger for the ejector cooling cycle.
- Among the investigated chiller technologies, the hybrid ejector and the electrical system represent the most economically convenient solutions. The convenience in the use of the hybrid ejector cycle strongly depends on the climatic zone and on the electric energy price. Solution C was always economically advantageous in moderate climatic zones such as Milan, whereas in climatic zones with a high cooling load, the hybrid ejector cooling systems were more convenient compared to electrical chillers after an acceptable economic lifetime (after 7.1 years in Madrid with 0.30 €/kWh electricity unit price, and after 9.5 years in Athens with 0.10 €/kWh electricity unit price). Scenarios with higher electricity costs made heat-driven cooling systems as the

ejector more and more economically advantageous compared to electrically driven technologies.

Finally, we would like to note that the hybrid multi-ejector system represents a brand-new technology within this range of climatization sizes, with an absent space in the marketplace and only few prototypes or related studies in the scientific literature. For this reason, some hypotheses related to component performance may influence the presented results with respect to real cases. Nevertheless, the benefits of the proposed optimized system when compared to conventional technologies were clearly shown and could not be affected by the uncertainty of the chosen assumptions.

Author Contributions: Conceptualization, A.W.M.; Investigation, G.L., G.N. and L.V.; Project administration, A.W.M.; Supervision, A.W.M.; Writing—Original draft, G.L. and G.N.; Writing—Review and editing, L.V. All authors have read and agreed to the published version of the manuscript.

Funding: This research received no external funding.

Institutional Review Board Statement: Not applicable.

Informed Consent Statement: Not applicable.

Conflicts of Interest: The authors declare no conflict of interest. The funders had no role in the design of the study; in the collection, analyses, or interpretation of data; in the writing of the manuscript, or in the decision to publish the results.

Nomenclature

A	heat exchanger surface [m ²]
A_m	ejector mixing section [m ²]
A_r	ejector area ratio [m ²]
A_t	ejector motive nozzle throat section [m ²]
AHP	absorption chiller
c_{el}	electricity unit price [€ kWh _{el} ⁻¹]
COP	coefficient of performance
EER	energy efficiency ratio
D	diameter [m]
E_{el}	electrical energy consumption [kWh]
EHP	electrical chiller
GWP	Global Warming Potential [kgCO _{2eq} kg ⁻¹]
h	specific enthalpy [kJ kg ⁻¹]
IC	investment costs [k€]
k	heat capacity ratio
\dot{m}	mass flow rate [kg s ⁻¹]
N	hours number
Nu	Nusselt number
ODP	Ozone Depletion Potential
ORC	Organic Rankine Cycle
p	pressure [bar]
Q	thermal energy [kWh]
\dot{Q}	thermal power [kW]
R	ideal gas constant [kJ kg ⁻¹ K ⁻¹]
RC	running costs [k€]
SEER	seasonal energy efficiency ratio
T	temperature [K]
TC	total costs [k€]
u	velocity [m s ⁻¹]
U	overall heat transfer coefficient [W m ⁻² K ⁻¹]

Greek

\dot{V}	volumetric flow rate [$\text{m}^3 \text{s}^{-1}$]
VCC	vapor compression cycle
W	energy consumption [kWh]
\dot{W}	power consumption [kW]
α	convective heat transfer coefficient [$\text{W m}^{-2} \text{K}^{-1}$]
β	ejector compression ratio
δ	thickness [m]
Δ	difference
ε	heat exchanger efficiency
η	efficiency
θ	time [hr]
κ	thermal conductivity [$\text{W m}^{-1} \text{K}^{-1}$]
μ	entrainment ratio
Π	pressure lift
ϕ	multi-ejector geometric scale

Subscript

<i>air</i>	related to the air
<i>amb</i>	external ambient
<i>build</i>	related to the building
<i>cb</i>	breakdown condition
<i>cc</i>	critical condition
<i>co</i>	condenser
<i>cold</i>	cold side
<i>D</i>	diffuser
<i>ej</i>	ejector
<i>el</i>	electrical
<i>ev</i>	evaporator
<i>f</i>	related to secondary fluid
<i>fan</i>	fans
<i>fluid</i>	related to the fluid
<i>gl</i>	global
<i>gv</i>	vapor generator
<i>h</i>	hydraulic
<i>hot</i>	hot side
<i>M</i>	mixing chamber
<i>m</i>	mixing section
<i>mat</i>	material
<i>max</i>	maximum value
<i>nom</i>	nominal
<i>N</i>	motive nozzle
<i>out</i>	outlet section
<i>over</i>	oversized conditions
<i>p</i>	refrigerant pump
<i>pf</i>	primary flow
<i>R</i>	rank
<i>ref</i>	related to the refrigerant
<i>rhe</i>	regenerative heat exchanger
<i>s</i>	isentropic
<i>sf</i>	secondary flow
<i>t</i>	motive nozzle throat section
<i>th</i>	thermal
<i>tot</i>	total
<i>under</i>	undersized conditions
<i>user</i>	final user

Appendix A

Table A1. Main sizing parameters of the heat exchangers.

High Pressure Evaporator Plate Heat Exchanger		Condenser Plate Fin and Tube		Low Pressure Evaporator One Pass Flooded Evaporator	
Plate height [mm]	to calculate	Tube length [mm]	to calculate	Tube length [mm]	to calculate
Channel number [#]	to calculate	Fin step [mm]	3 ÷ 6	Tube number	to calculate
Plate width [mm]	150	Fin thickness [mm]	0.1/0.2	External tube diameter [mm]	4.0
Plate spacing [mm]	0.5	Tube pitch [mm]	33	Tube thickness [mm]	0.4
Wavelength corrugation [mm]	1.0	Rank pitch [mm]	33	Baffle spacing [mm]	250.0
Chevron angle [°]	80	Tube number [#]	20/25/30	Shell diameter [mm]	140.0
Plate thickness [mm]	0.2	Tube external diameter [mm]	8.0		
		Tube thickness [mm]	1.0		
		Rank number [#]	3 ÷ 6		

References

- International Energy Agency. *World Energy Outlook*; International Energy Agency: Paris, France, 2014.
- International Energy Agency. *Energy Technology Perspectives: Scenarios & Strategies to 2050*; International Energy Agency: Paris, France, 2010.
- European Commission. *Mapping and Analysis of the Current and Future (2020–2030) Heating/Cooling Fuel Deployment (Fossils/Renewables)*; European Commission: Brussels, Belgium, 2016.
- IEA, International Energy Agency. Data and Statistic. Explore Energy Data by Category, Indicator, Country or Region. Available online: <https://www.iea.org/data-and-statistics?country=EU28&fuel=Energy%20supply&indicator=Electricity%20generation%20by%20source> (accessed on 29 August 2020).
- GSE. Monitoraggio Statistico Degli Obiettivi Nazionali e Regionali Sulle FER-Anni 2012–2018. Available online: <https://www.gse.it/dati-e-scenari/statistiche> (accessed on 24 August 2020).
- Besagni, G.; Mereu, R.; Inzoli, F. Ejector refrigeration: A comprehensive review. *Renew. Sustain. Energy Rev.* **2016**, *53*, 373–407. [CrossRef]
- Sun, D.W. Comparative study of the performance of an ejector refrigeration cycle operating with various refrigerants. *Energy Convers. Manag.* **1999**, *40*, 873–884. [CrossRef]
- Kasperski, J.; Gil, B. Performance estimation of ejector cycles using heavier hydrocarbon refrigerants. *Appl. Therm. Eng.* **2014**, *71*, 197–203. [CrossRef]
- Chen, J.; Havtun, H.; Palm, B. Screening of working fluids for the ejector refrigeration system. *Int. J. Refrig.* **2014**, *47*, 1–14. [CrossRef]
- Gil, B.; Kasperski, J. Efficiency analysis of alternative refrigerants for ejector cooling cycles. *Energy Convers. Manag.* **2015**, *94*, 12–18. [CrossRef]
- Lillo, G.; Mastrullo, R.; Mauro, A.W.; Trinchieri, R.; Viscito, L. Thermo-economic analysis of a hybrid ejector refrigerating system based on a low grade heat source. *Energies* **2020**, *13*, 562. [CrossRef]
- Sun, D.W. Variable geometry ejectors and their applications in ejector refrigeration systems. *Energy* **1996**, *21*, 919–929. [CrossRef]
- Pereira, P.R.; Varga, S.; Oliveira, A.C.; Soares, J. Development and performance of an advanced ejector cooling system for a sustainable built environment. *Front. Mech. Eng.* **2015**, *1*, 7. [CrossRef]
- Van Nguyen, V.; Varga, S.; Soares, J.; Dvorak, V.; Oliveira, A.C. Applying a variable geometry ejector in a solar ejector refrigeration system. *Int. J. Refrig.* **2020**, *113*, 187–195. [CrossRef]
- Chen, J.; Havtun, H.; Palm, B. Investigation of ejectors in refrigeration system: Optimum performance evaluation and ejector area ratios perspectives. *Appl. Therm. Eng.* **2014**, *64*, 182–191. [CrossRef]
- Shestopalov, K.O.; Huang, B.J.; Petrenko, V.O.; Volovyk, O.S. Investigation of an experimental ejector refrigeration machine operating with refrigerant R245fa at design and off-design working conditions. Part 2. Theoretical and experimental results. *Int. J. Refrig.* **2015**, *55*, 212–223. [CrossRef]
- McLinden, M. *Reference Fluid Thermodynamic and Transport Properties, Nist Standard Reference Database 23; Version 9.1*; Physical and Chemical Properties Division, NIST: Gaithersburg, MD, USA, 2002.
- Declaye, S. Vincent Lemort, Improving the Performance of μ -ORC Systems. Ph.D. Thesis, Université de Liège, Liège, Belgium, 2015.
- Varga, S.; Lebre, P.S.; Oliveira, A.C. Readdressing working fluid selection with a view to designing a variable geometry ejector. *Int. J. Low Carbon Technol.* **2015**, *10*, 205–215. [CrossRef]
- TRNSYS 17, a TRAnSient System Simulation Program; Solar Energy Laboratory, University of Wisconsin-Madison: Madison, WI, USA, 2010. Available online: <http://www.trnsys.com/index.html> (accessed on 29 August 2021).
- Cecchinato, L.; Chiarello, M.; Corradi, M. A simplified method to evaluate the seasonal energy performance of water chillers. *Int. J. Therm. Sci.* **2010**, *49*, 1776–1786. [CrossRef]

-
22. Kühn, A. (Ed.) *Thermally Driven Heat Pumps for Heating and Cooling*; Universitätsverlag der TU Berlin: Berlin, Germany, 2013.
 23. Berliner Energieagentur GmbH. *Meeting Cooling Demands in Summer by Applying Heat from Cogeneration*; Summerheat Publishable Report; Berliner Energieagentur GmbH: Berlin, Germany, 2009.